EXPERIMENTAL AND NUMERICAL STUDY OF STRENGTHENED HINGED FRAMES USING CFRP

Hesham F. Shaaban*

ABSTRACT

In this research, a study of strengthened hinged one-storey frames subjected to four-point loading, both experimentally and numerically, is presented. Three full scale hinged frames with dimensions 2400 mm (span) and 1200 mm (height) are tested in this study. The concrete reinforced frames are strengthened using CFRP sheets at locations of sagging and hogging moments. One specimen is strengthened for shear stress, using external CFRP shear laminates, in addition to sagging and hogging moments locations. A non-linear analysis for the tested hinged frames using ANSYS software package is also presented. The strengthened specimens achieved considerable improvement by increasing both; failure load, especially for the third specimen. The results have been confirmed by the proposed numerical model which revealed other important results concerning the strengthening scheme.

Keywords: RC Frames, CFRP, finite element analysis, retrofitting, strength, rehabilitation.

INTRODUCTION

In recent years, there has been an increased need in strengthening and repairing existing concrete structures, and this process requires a vast monetary investment. Therefore, today there is a need to investigate appropriate and economical alternative to strengthen and to repair existing concrete structures. Bonding external steel plates; and using advanced composite materials Fiber Reinforced Polymer (FRP) are among these alternatives.

The use of fiber reinforced polymers (FRPs) was found to be an effective alternative with rapid retrofit time and providing substantial increase in strength with limited ductility. The performance of FRP was influenced mainly by two important parameters: the ratio of FRP bond length in shear span to concrete depth and the ratio of laminate stiffness to tension reinforcement stiffness. The efficiency of (FPR) increases with the increase in bond length (or the first ratio) and decreases with the amount of FRP laminates (or the second ratio), [7], [8].

***Structural Engineering Dept., University of zagazig, Zagazig, Egypt, Canada**

The debonding failure load depends strongly on the stiffness of the "composite plate" composed of the bonded plate and the concrete cover or the bonded plate alone. For plate ends subjected to a high shear force and a low moment, cover separation failure often occurs following local shear-crack induced interfacial debonding between the plate and the concrete near the plate end. The shear resistance contributed by the concrete alone provides a lower bound to the debonding failure load of such plate ends, which can be significantly increased by the presence of external CFRP shear laminates, [3], [4], and [9].

Numerous trials were carried out by several researchers to prevent the premature peeling failure at the ends. Among these applied techniques are: concrete cover replacement by grout to enhance the resistance of substrate to crack initiation and propagation and the continuation of the CFRP plate under the support. In the third technique, permanent compressive forces at the ends of bonded plate are applied using different plate end

anchorage systems, i.e. end anchorage by bolts or by mechanical clamps, [2], [10], and [11].

EXPERIMENTAL PROGRAM

Test frame details

A total of three reinforced concrete full-scale hinged frames with dimensions 2400 mm (span), 1200mm (height) and150 (thickness) were cast and tested in the Structures Lab, Faculty of Engineering, Zagazig University under four-point loading. All the frames were reinforced with 2Φ 12 mm as main and secondary steel. Mild steel stirrups of 8 ? 8 mm/m were used to resist shear stress.

Figure (1) shows the dimensions and reinforced steel details of the control specimen (Fcont).

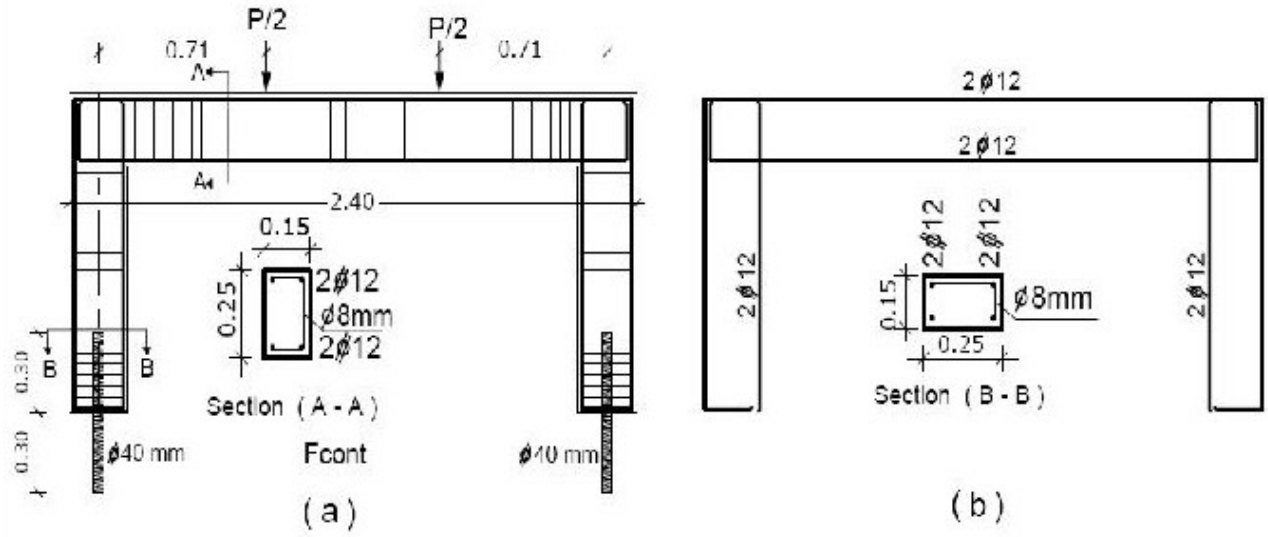

Fig. 1- Dimensions and Reinforced Steel Details of Control Specimen

A tension test was performed on three pieces of the reinforcing bars, each of length 500 mm. The average yield stress was 360 N/mm^2, while the average ultimate tensile strength was 560 N/mm^2. Six concrete cubes of side length of 150 mm were prepared at the time of casting and were kept with the beams during curing process.

The average 28-day concrete cube strength f_{cu} was 29 MPa. A threaded bar Φ 40 mm was welded to the reinfor-ced steel rig of the two frame ends to achieve the hinge support conditions.

In the sagging moment two layers of CFRP were applied, while in hogging moment regions only one layer of CFRP was used. The details of the CFRP arrangement for the two frames (FRP1 and FRP2) are shown in Fig. (2).

In strengthened frame FRP1, one of the two CFRP layers' located in bottom face of the beams' frame was extended over the beam-column soffit to cover about 15 cm of the frame leg, in a trial to avoid CFRP debonding.

While, in the second strengthened frame FRP2, the two layers of the CFRP were terminated just before the soffit of the frame legs. This difference in arrangement of the CFRP end condition in the two specimens is to study the effect of continuation of the CFRP plate on the behavior and failure mode. Also, additional CFRP vertical stirrups were glued in shear zones to enhance the shear strength of the frame and achieve maximum efficiency of the strengthening system.

The CFRP material consisted of 100 mm wide, and 0.12 mm thick carbon laminates. The sheets were externally bonded to the tension face of the concrete using a two-part epoxy of Sikadur-330 mixed at ratio of 4:1 by weight and cured at room temperature. The tensile strength of fiber was 4100 N/mm^2, tensile E-modulus of fibers was 231,000 N/mm^2 and the strain at break of fibers was 1.7%. The fabric design thickness of each layer of the CFRP strips was 0.12 mm based on total carbon content and the density was 1.78g/cm^3.

Test set-up and loading procedure

The typical set-up used in the experimental program is shown in Fig. (3). As the total hinged frame length is 2.4 m, the span of rigid frame

(distance between threaded steel bar 40mm diameter at frames' legs centre) is 2.15 m. To achieve the hinge support condition at the two ends, the threaded bars which were welded to the reinforcement rigs of the frame columns, are clamped to steel set-up frame. The load was applied at two-point load using a hydraulic jack against the rigid set-up steel frame with a constant rate up to failure. The two load points were offset by 370 mm from the mid-span of the frame, as illustrated in Fig. (3). The load was progressively increased up to failure of the specimens when no further load could be sustained. Vertical deflections were measured by LVDT transducers placed under load points, and at mid span. Horizontal displacements were also measured at the top surface of the frame. Tensile strains of the CFRP laminates and also the compressive strains of the concrete were measured at mid span. The load, deflections and strains were recorded every load step (5 KN). Before the commencement of each test, a small load was applied to check the specimen set-up, instrumentation and the loading system.

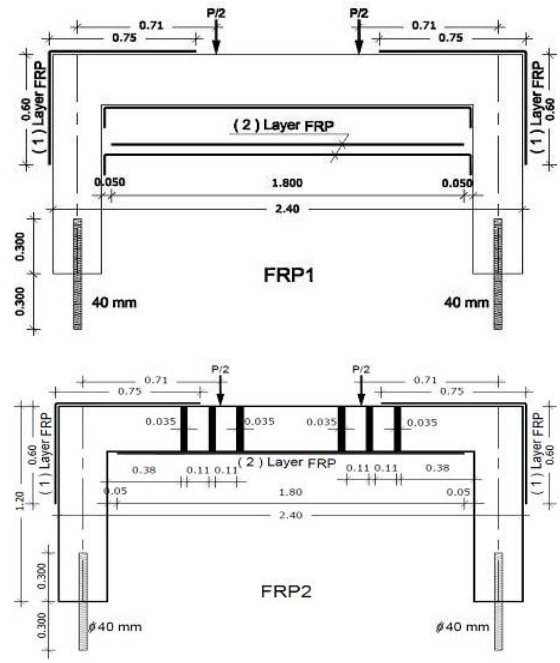

Fig. 2- Details of CFRP Arrangements for Frames FRP1 and FRP2

Fig. 3- Test set-up

EXPERIMENTAL RESULTS

The failure load and modes of failure of all tested frames are summarized in Table (1). For the strengthened frames (FRP1 and FRP2), an increase in the load-carrying capacity were recorded when CFRP external sheets were added. The percentages of the failure load increase are 24% and 37% for FRP1 and FRP2, respectively. For the control

specimen (Fcont) firstly, yielding of the tensional steel reinforcement in the pure flexural zone (between the two loading points) took place, then followed by failure in the concrete beam due to the shear stress accompanied with flexural stress under the point load; as illustrated in Fig. (4).

Table 1- Results of the tested frames

Label	Strengthed region	Load (KN)	Δy (mm)	Δu (mm)	Mode of failure
Fcont	Control specimen	113	3.3	6.6	Concrete shear/flexural
FRP1	Positive & Negative moments	140	5.24	8.45	Concrete shear failure/ Rupture in FRP
FRP2	Positive, negative moments and shear	155	5.22	8.76	Concrete shear failure/Concrete cover separation

Fig. 4- Failure of Control Specimen Fcont due to Concrete Shear Failure

For the specimen frame (FRP1), strengthening the flexural moment resistance by CFRP sheets, succeeded in delaying the failure which finally occurred in the same manner as that of the control specimen. Diagonal shear cracks started under the load point and propagated widely causing shear cut of the CFRP sheets at failure load; as illustrated in Fig. (5). It worth mentioning, that the continuity of one of the CFRP sheet over the frame legs succeeded to prevent the end plate peeling mode.

For the third specimen frame (FRP2) strengthened in shear zones by CFRP stirrups in addition to flexural, diagonal shear cracks started under the load points. Then and due to the presence of CFRP stirrups, theses cracks didn't propagate. Finally, and after an increase in applied load by about 37% compared to the control frame, the specimen failed in shear.

Upon failure, the cracks were recorded just after the third CFRP shear stirrup causing shear failure. At the end of the CFRP sheets, failed in concrete cover separation mode, as could seen in Fig. (6).

This failure mode is logic as the CFRP sheets was not continuous over the frame legs as specimen FRP1.

Figeure. (7) shows loads versus deflection at mid-span for tested specimens. Deflections of the streng-thened specimens were reduced under the same load as compared with the reference test by about 6.5% and 21%.

The deflections corresponding to the yielding load and ultimate load are defined as yielding deflection Δy and ultimate deflection Δu, respectively. The ductility is defined as the ratio of ultimate deflection Δu to yielding deflection Δy.

The ductility of strengthened frames has a range of 1.61 to 1.68 compared to 2.0 for the control specimen case.

The low ductility of strengthened specimens indicates that the addition of CFRP as reinforcement greatly reduces the deforming ability at the ultimate stage of loading.

Fig. 5- Failure of Specimen FRP1 due to Concrete Shear Failure

Fig. 6- Failure of Specimen FRP2 due to Concrete Shear Failure Followed by Concrete Cover Separation

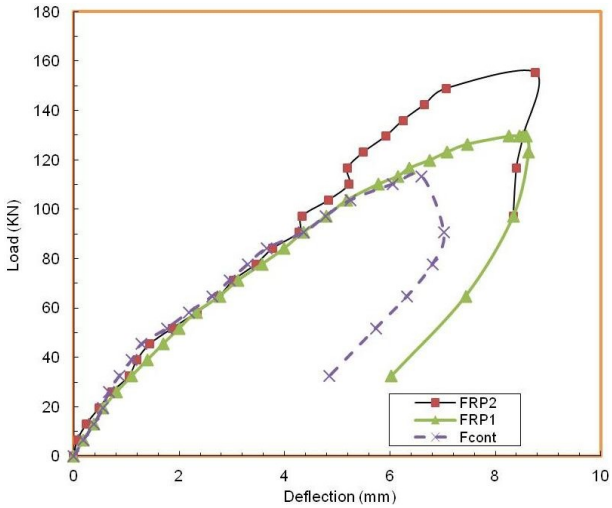

Fig. 7 Load-Deflection Curves for Tested Specimens

Fig. (8) shows the load strain curves at mid-span of the positive steel reinforcement of the tested specimens.

It can be seen that each curve consists of three straight lines with different slopes.

The first turning point indicates the cracking of concrete in tension zone.

The second turning point refers to the yielding of tension steel.

The yielding and maximum loads can be found for each specimen from its load-strain curve. Strains of the steel reinforcement for the strengthened frames are reduced under the same load as compared with the reference frame with values ranged from 10% to 90%.

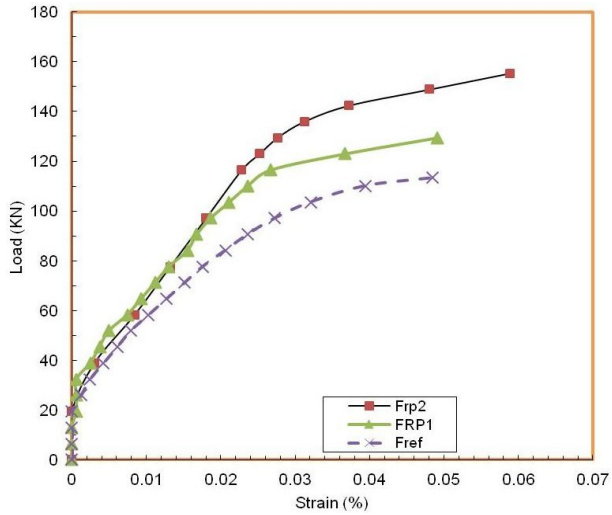

Fig. 8 Load-strain Curves of Positive Steel for Tested Specimens

Numerical Analysis

Software, element types and mesh construction

In the present study, the finite element program ANSYS was utilized to simulate the behaviour of the reinforced concrete frames and CFRP.

A three dimensional finite element model was presented to simulate the material non-linear behaviour of the tested frames. The used elements are summarized in the following lines, [1].

The concrete section was modelled using a three-dimensional concrete element (solid 65). The most important aspect of this element is the treatment of the non-linear material properties. The concrete is capable of cracking (in three orthogonal directions), crushing, plastic deformation and creep. The steel reinforcement was simulated by a three-dimensional spar element (link 8) embedded in the concrete. Using this separate spar element for representing steel reinforcement in the concrete section allowed the bars to be placed in their exact position.

Layered solid (SOLID46) element was used to represent the CFRP strips. The element allows up to 250 different material layers with different orientations and orthotropic material properties in each layer.

The element has three degrees of freedom at each node and translations in the nodal x, y and z directions. A typical finite element mesh for the tested frame is shown in Fig. (9).

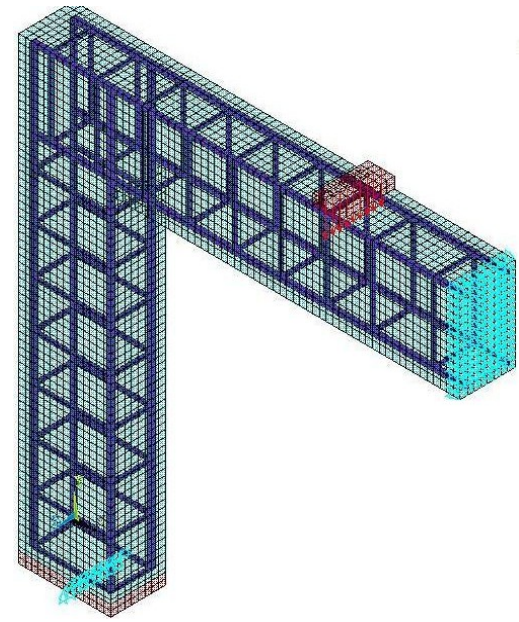

Fig. 9 Finite Element Mesh for RC Frame Model

Material modelling

In the proposed concrete material model, the stress-strain curve for concrete is linearly elastic up to about 30 percent of the maximum compressive strength; as shown in Fig. (10).

Above this point, the stress increases gradually up to the maximum compressive strength. In tension, the stress-strain curve for concrete is approximately linearly elastic up to the maximum tensile strength. After this point, the concrete cracks and the strength decrease steeply to zero tension stress.

Relaxation coefficient, shear transfer for open and closed cracks, and concrete crushing were considered. For steel reinforcement bars, the stress-strain curve was represented using a tri-linear relationship as shown in Fig. (11). Sufficient accuracy was achieved by using this relationship.

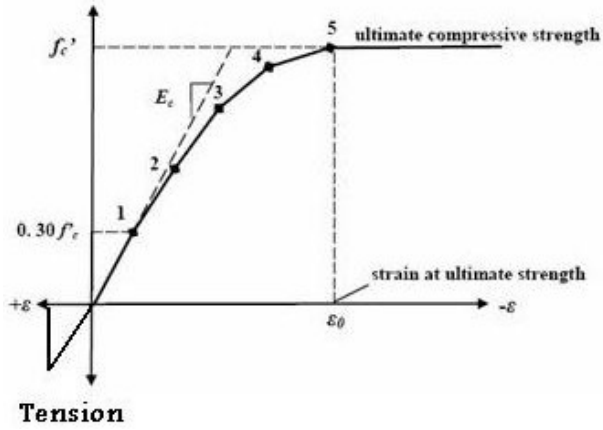

Fig.10. Stress-strain curve for concrete

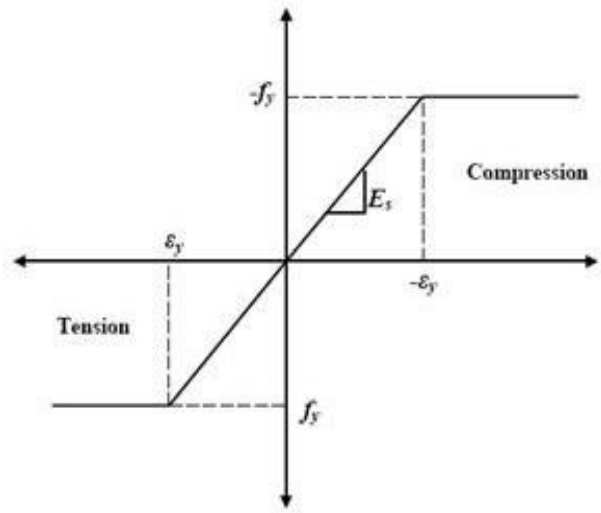

Fig. 11. Stress-strain curve for steel bars

The FRP composites are an isotropic material; that is, their properties are not the same in all directions.

The unidirectional lamina has three mutually orthogonal planes of material properties. The xyz coordinate axes are referred to as the principal material coordinates where the x direction is the same as the fiber direction, and the y and z directions are perpendicular to the x direction.

It is a so-called especially orthotropic material, [5], [6]. Linear elastic properties of the FRP compo-sites were assumed throughout this study.

Material properties of all the used materials were taken as the experimental materials for the finite element model.

Perfect bond between concrete and steel reinforcement bars was assumed since the bond between them is not a point of concern in this study.

To provide this bond, the link element for the steel reinforcing was connected between nodes of each adjacent concrete solid element, so the two materials shared the same nodes.

The same approach was adopted for FRP composites. For simplicity, and due to the high strength of the epoxy and its thin layer used to attach FRP sheets to the experimental frames supported the perfect bond assumption.

Comparison between numerical and experimental results

Comparison between the experimental and the finite element results presented to check the accuracy of the finite element simulation when CFRP strips are used.

The general behaviour of the finite element models represented by the load-deflection plots at mid-span show good agreement with the test data; as shown in Figures (12 and 13).

However, the finite element models show slightly higher stiffness than the test data in both the linear and nonlinear ranges.

The effects of bond slip (between the concrete and steel reinforcing), microcracks occurring in the actual beams were excluded in the finite element models and due to the full bond considered between the CFRP and the concrete in the finite

element model for streng-thened frames (FRP1 and FRP2) while in the experimental test 100% bond cannot be reached perfectly contributing to the higher stiffness of the finite element models.

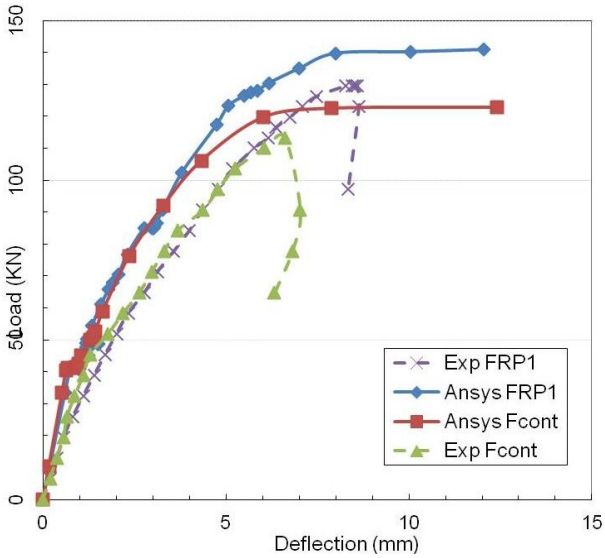

Fig. 12 Experimental and Numerical results for Fcont and FRP1 frames

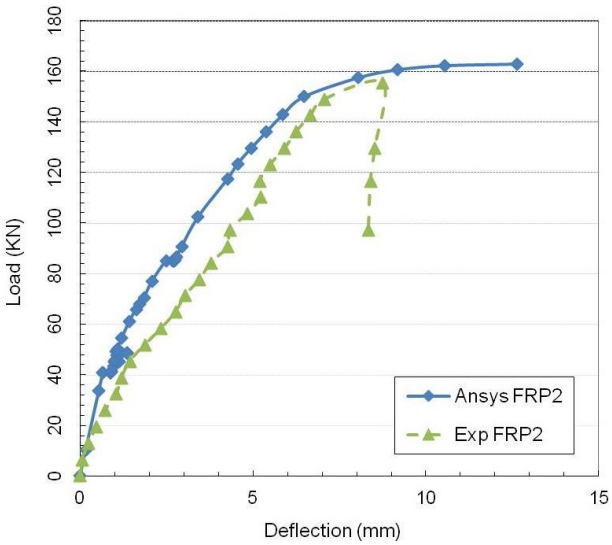

Fig. 13 Comparison between experimental and Numerical results for FRP2 frame

Figure (14) shows the cracks and crushing output of the ANSYS model for control specimen Fcont almost at failure.

The diagonal cracks shown in red colour represent the shear cracks which were distributed in shear zones.

The horizontal cracks appeared in green colour could be seen between point loads.

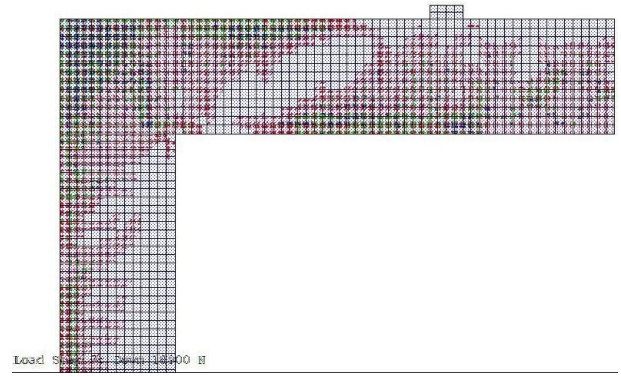

Fig. 14 Cracks distribution of specimen Fcont at failure

CONCLUSIONS

Based to the results obtained from this research, it could be concluded that:-

Strengthening RC frame with CFRP sheets in flexure FRP1 increased the load carrying capacity of the frames by 24%.

Strengthening the frame FRP2 by CFRP sheets in shear zones in addition to flexure, increased the load carrying capacity by 37%, and succeeded to shift the shear failure mode away of strengthened area.

Extending the CFRP sheets over the frames legs succeeded to prevent the end plate peeling mode.

The FE presented in this paper has shown remarkable features of simplicity of use and reasonable accuracy in the representation of the mechanical behaviour of RC structures, FRP-strengthened for flexure and shear.

REFERENCES

1- ANSYS Element Manual, Tenth Edition, Swanson Analysis System Inc., Pennsylvania, USA.

2- Buyukozturk, O., Gunes, O. and Karca, E., "Progress on Understanding Debonding Problems in Reinforced Concrete and Steel Members Strengthened Using FRP Composites", Constr. Build. Mat, (2004), 18(1), p 9-19.

3- El-Shihy, A.M., Fawzy, H.M., Mustafa, S.A. and El-Zohairy, A.A. "Experimental and Numerical Analysis of Composite Beams Strengthened by CFRP" Steel and Composite Structures, (2010), Vol. 10, No. 3, p 439.

4- Gao, B., Leung, C.K.Y. and Kim, J.K., "Failure Diagrams of FRP Strengthened RC Beams", J. Compos. Struct., (2005), p 1-16.

5- Gibson, R.F., Principles of Composite Material Mechanics, McGraw-Hill, Inc., New York, (1994).

6- Kaw, A.K., Mechanics of Composite Materials, CRC Press LLC, Boca Raton, Florida, (1997) .

7- Li, L.J., Guo, Y.C., Liu, F. and Bungey, J.H., "An Experimental and Numerical Study of the Effect of Thickness and Length of CFRP on Performance of Repaired Reinforced Concrete Beams", J. Constr. Build. Mat., (2006), 20(10), p 901-909.

8- Pham, H.B. and Al-Mahaidi, R., "Experimental Investigation Into Flexural Retrofitting of Reinforced Concrete Bridge Beams Using FRP Composites", Composite Structures, (2004), Vol. 66, No. 1-4, p 617.

9- Shield, C., French, C., and Milde, E., "The Effect of Adhesive Type on the Bond of NSM Tape to Concrete", Proc. Of FRPRCS-7 Symp., Eds T. Triantafillou, Greece, (2006).

10- Sallam, H.E.M. , Saba, A.M., Shaheen, H.H., and Abdel-Raouf, H., "Prevention of Peeling Failure in Plated Beams" J. Adv. Conc. Techn., (2004), Vol. 2, No.3, p 419.

11- Yao, J., and Teng, J.G., " Plate end Debonding in FRP-plated RC Beams—I: Experiments", Engng. Structure, ASCE, (2007), Vol. 29, p 2457.